WILEY InterScience® DISCOVER SOMETHING GREAT

PROTEINS STRUCTURE ■ FUNCTION ■ BIOINFORMATICS

SHORT COMMUNICATION

Identification and structural characterization of heme binding in a novel dye-decolorizing peroxidase, TyrA

Chloe Zubieta,[1,2] Rosanne Joseph,[2] S. Sri Krishna,[1,3,4] Daniel McMullan,[1,5] Mili Kapoor,[6] Herbert L. Axelrod,[1,2] Mitchell D. Miller,[1,2] Polat Abdubek,[1,5] Claire Acosta,[1,5] Tamara Astakhova,[1,4] Dennis Carlton,[1,6] Hsiu-Ju Chiu,[1,2] Thomas Clayton,[1,6] Marc Deller,[1,6] Lian Duan,[1,4] Ylva Elias,[1,6] Marc-André Elsliger,[1,6] Julie Feuerhelm,[1,5] Slawomir K. Grzechnik,[1,4] Joanna Hale,[1,5] Gye Won Han,[1,6] Lukasz Jaroszewski,[1,3,4] Kevin K. Jin,[1,2] Heath E. Klock,[1,5] Mark W. Knuth,[1,5] Piotr Kozbial,[1,3] Abhinav Kumar,[1,2] David Marciano,[1,6] Andrew T. Morse,[1,4] Kevin D. Murphy,[1,6] Edward Nigoghossian,[1,5] Linda Okach,[1,5] Silvya Oommachen,[1,2] Ron Reyes,[1,2] Christopher L. Rife,[1,2] Paul Schimmel,[6] Christina V. Trout,[1,6] Henry van den Bedem,[1,2] Dana Weekes,[1,3] Aprilfawn White,[1,5] Qingping Xu,[1,2] Keith O. Hodgson,[1,2] John Wooley,[1,4] Ashley M. Deacon,[1,2] Adam Godzik,[1,3,4] Scott A. Lesley,[1,5,6] and Ian A. Wilson[1,6]*

[1] Joint Center for Structural Genomics (JCSG)

[2] Stanford Synchrotron Radiation Laboratory, Stanford University, Menlo Park, California

[3] Burnham Institute for Medical Research, La Jolla, California

[4] Center for Research in Biological Systems, University of California, San Diego, La Jolla, California

[5] Genomics Institute of the Novartis Research Foundation, San Diego, California

[6] The Scripps Research Institute, La Jolla, California

ABSTRACT

TyrA is a member of the Dye-decolorizing Peroxidase (DyP) family, a new family of heme-dependent peroxidase recently identified in fungi and bacteria. Here, we report the crystal structure of TyrA in complex with iron protoporphyrin (IX) at 2.3 Å. TyrA is dimeric, with each monomer exhibiting a two-domain, α/β ferredoxin-like fold. Both domains contribute to the heme-binding site. Co-crystallization in the presence of an excess of iron protoporphyrin (IX) chloride allows for the unambiguous location of the active site and the specific residues involved in heme binding. The structure reveals a Fe-His-Asp triad essential for heme positioning, as well as a novel conformation of one of the heme propionate moieties. Structural comparison to the canonical DyP family member, DyP from Thanatephorus cucumeris *(Dec 1), demonstrates conservation of the novel heme conformation, as well as residues important for heme binding. Structural comparisons with representative members of all classes of the plant, bacterial, and fungal peroxidase superfamily demonstrate that TyrA, and by extension the DyP family, adopts a fold different from all other structurally characterized heme peroxidases. We propose that a new superfamily be added to the peroxidase classification scheme to encompass the DyP family of heme peroxidases.*

Proteins 2007; 00:000–000.

Key words: heme-binding protein; heme conformation; peroxidase; structural genomics; DyP; X-ray crystallography.

Grant sponsor: National Institutes of Health, Protein Structure Initiative; Grant numbers: P50 GM62411, U54 GM074898, GM15539.
*Correspondence to: Dr. Ian Wilson, The Scripps Research Institute, BCC206, 10550 North Torrey Pines Road, La Jolla, CA 92037. E-mail: wilson@scripps.edu
Received 15 May 2007; Accepted 12 June 2007
Published online 00 Month 2007 in Wiley InterScience (www.interscience.wiley.com). DOI: 10.1002/prot.21673

J_ID: Z7E Customer A_ID: 21673 Cadmus Art: PROT21673 Date: 28-JUNE-07 Stage: I Page: 2

INTRODUCTION

Peroxidases are ubiquitous enzymes used by all living organisms for biosynthesis, degradation, defense, and mediating a response to oxidative stress. Isolated from animals, plants, bacteria, and fungi, peroxidases are subdivided into two superfamilies, namely, the plant peroxidases, which include the bacterial and fungal peroxidases,[1] and the animal peroxidases.[2,3] The plant peroxidase superfamily is further subdivided into three classes based on biological origin (bacterial, archaeal, and fungal) and sequence alignment.[1] Class I plant peroxidases are intracellular peroxidases of prokaryotic lineage with no disulfides or ion-binding sites, and include yeast cytochrome c peroxidase (CcP).[4] Class II are predominantly extracellular and are secretory fungal peroxidases,[5] and include lignin peroxidase (LiP)[6] and manganese peroxidase (MnP).[7] Class III peroxidases, such as horseradish peroxidase (HRP), are largely extracellular and of plant origin.[8,9] The class II and III plant peroxidases have two conserved calcium ion-binding sites on the distal and proximal domains and four nonconserved disulfide bridges. All three classes of the plant peroxidase superfamily are two-domain, predominantly α-helical proteins lacking any extensive β structure, with both domains contributing to the active site. The N-terminal domain contributes the distal histidine residue important for heme binding, while the larger C-terminal domain contributes the proximal ligands to sequester heme. The two domains form an active site crevice, with a heme molecule sandwiched between α-helices. The animal peroxidase superfamily is unrelated to the plant superfamily based on primary and tertiary structure, and consists of largely α-helical, multidomain proteins as represented by the structure of myeloperoxidase.[2]

While structurally distinct, all heme-dependent peroxidases generate a reactive iron-oxo species in order to oxidize a wide variety of substrates. The reaction proceeds via Compound I, an oxidized intermediate oxoferryl ($Fe(IV)=OR^{\cdot}$) species[10] and porphyrin radical,[11,12] or protein-based radical cation,[13] according to the following reaction scheme.

$$\text{Peroxidase}\,(Fe^{3+}) + H_2O_2 \rightarrow (Fe^{4+})=OR^{\cdot}\,(\text{Compound I}) + H_2O$$

$$(Fe^{4+})=OR^{\cdot}\,(\text{Compound I}) + \text{substrate} \rightarrow (Fe^{4+})=OR\,(\text{Compound II}) + \text{oxidized substrate}$$

$$(Fe^{4+})=OR\,(\text{Compound II}) + \text{substrate} \rightarrow \text{Peroxidase}(Fe^{3+}) + H_2O + \text{oxidized substrate}$$

This two-electron process reduces peroxide to water, and the two oxidizing equivalents are used to oxidize one or more substrate molecules.

Recently, a distinct family of heme-dependent peroxidase from fungi has been identified. The DyP (for dye decolorizing peroxidase) family constitutes a novel class of plant peroxidase and includes canonical members such as DyP from *Thanatephorus cucumeris* Dec 1 (formerly called *Geotrichum candidum* Dec 1)[14] and TAP from *Termitomyces albuminosus*.[15] Because these enzymes were derived from fungal sources, the DyP family was thought to be structurally related to the class II secretory fungal peroxidases. However, members of the DyP family do not exhibit significant sequence identity to classical fungal peroxidases, such as LiP and MnP, and do not contain the conserved proximal and distal histidines and catalytically essential arginine found in other plant peroxidase superfamily members.[1] Available structures of related heme-binding proteins, such as TT1485,[16] and two DyP family members, DyP[17] and *Bt*DyP,[18] reveal a β-barrel ferrodoxin-like fold, which is distinct from all structurally characterized peroxidases to date. Results from mutagenesis studies,[19] computational docking,[17] and sequence comparisons[16,20] differ in the mode of heme binding and even in the location of the heme-binding site. Concurrent with our studies, the crystallographic coordinates of DyP in complex with heme (PDB accession code 2d3q) have been released, supporting our results for heme-binding motifs.[18] Here, we report the structure of TyrA from *Shewanella oneidensis* (strain MR-1) (PDB accession code 2iiz) in its heme-bound form, and describe the novel heme conformation and residues important for sequestration of the heme molecule. In addition, we compare the heme/TyrA complex to the structure of apo TyrA[18] and to structural representatives of class I, II, and III plant peroxidases.

MATERIALS AND METHODS

Protein production and crystallization

Protein production is described in Zubieta *et al.*[18] The TyrA/heme complex was crystallized using a 2-μL (1 μL protein solution + 1 μL crystallization solution) hanging drop, with a crystallization reagent containing 0.1*M* Tris pH 8.0, 5% (v/v) 2-propanol, 20% (w/v) polyethylene glycol 4000, and 1 m*M* hemin (Sigma Aldrich) at 288 K. Ethylene glycol was added as a cryoprotectant to a final concentration of 15%. The crystals were indexed in tetragonal space group $P4_32_12$ (Table I). T1

Data collection, structure solution, and refinement

Data for the heme-bound TyrA crystals were collected on SSRL beamline BL11-1 at a wavelength of 1 Å. The data sets were collected at 100 K using a Q315 ADSC CCD detector. The data were integrated and reduced using XDS[23] and then scaled with the program AQ3

DOI 10.1002/prot

ID: jaganm Date: 28/6/07 Time: 17:38 Path: J:/Production/PROT/Vol00000/070247/3B2/C2PROT070247

Table I
Summary of Crystal Parameters, Data Collection, and Refinement Statistics for TyrA/Heme Complex (PDB: 2iiz)

Space group	$P4_32_12$		
Unit cell parameters	$a = b = 94.84$ Å; $c = 116.67$ Å		
Data collection	λ_1		
Wavelength (Å)	1.0000		
Resolution range (Å)	19.9–2.30		
Number of observations	168,265		
Number of unique reflections	24,210		
Completeness (%)	99.7 (100.0)[a]		
Mean I/σ (I)	11.7 (3.0)[a]		
R_{sym} on I (%)	14.2 (55.2)[a]		
Highest resolution shell (Å)	2.45–2.30		
Model and refinement statistics			
Resolution range (Å)	19.8–2.30	Data set used in refinement	λ_1
No. of reflections (total)	24,207[b]	Cutoff criteria	$\|F\| > 0$
No. of reflections (test)	1269	R_{cryst}	0.205
Completeness (% total)	99.9	R_{free}	0.266
Stereochemical parameters			
Restraints (RMS observed)			
Bond angle (°)	1.36		
Bond length (Å)	0.013		
Average isotropic B-value (Å^2)	33.3		
ESU based on Rfree (Å)	0.21		
Protein residues/atoms	306/2446		
Water molecules/ligands	112/5		

ESU, Estimated overall coordinate error.[21,22]
$R_{sym} = \Sigma|I_i - \langle I_i\rangle|/\Sigma|I_i|$, where I_i is the scaled intensity of the i^{th} measurement and $\langle I_i\rangle$ is the mean intensity for that reflection.
$R_{cryst} = \Sigma|\,|F_{obs}| - |F_{calc}|\,|/\Sigma|F_{obs}|$, where F_{calc} and F_{obs} are the calculated and observed structure factor amplitudes, respectively.
R_{free} = as for R_{cryst}, but for 5.2% of the total reflections chosen at random and omitted from refinement.
[a]Highest resolution shell in parentheses.
[b]Typically, the number of unique reflections used in refinement is less than the total number that were integrated and scaled. Reflections are excluded due to systematic absences, negative intensities, and rounding errors in the resolution limits and cell parameters.

XSCALE.[23] The structure was solved by molecular replacement (MR) using the apo TyrA structure (PDB id: 2hag) with the program Phaser.[24] Completion and refinement of the model were performed in COOT[25] and REFMAC5,[26] respectively. Data and refinement statistics for the TyrA/heme structure are summarized in Table I.

Peroxidase activity assay

TyrA peroxidase activity was assayed by monitoring a decrease in absorbance at 600 nm using reactive blue 5 (RB5), a representative anthraquinone dye, as a substrate. Reactions were performed in 25 m*M* citrate buffer, pH 3.2, containing 100 μg of RB5, with a final volume of 1 mL. Different concentrations of TyrA (no TyrA, 0.1 μ*M*, 0.5 μ*M*, and 1 μ*M*) were added to the substrate solution followed by addition of H_2O_2 at a concentration of 0.2 m*M* to initiate the reaction. To calculate the K_m value for the reaction, varying concentrations of RB5 (0, 20, 40, 80, 120, 140, 200, 250, and 300 μ*M*) were added to a constant concentration of TyrA (1 μ*M*) and H_2O_2 (0.2 m*M*). The steady-state kinetic constants were estimated by fitting the data to the Michaelis-Menten equation. All reactions were performed in triplicate at room temperature.

Validation and deposition

Analysis of the stereochemical quality of the model was accomplished using AutoDepInputTool,[27] MolProbity,[21] SFcheck 4.0,[22] and WHATIF 5.0.[28] Atomic coordinates and experimental structure factors for heme-bound TyrA at 2.3 Å have been deposited in the PDB and are accessible under the code 2iiz.

RESULTS AND DISCUSSION

The crystal structure of heme-bound TyrA was determined to 2.3 Å by MR using the apo TyrA structure.[18] The final model of heme-bound TyrA includes a monomer (residues 5–310), one heme molecule, two ethylene glycol molecules, one 2-propanol molecule, one sodium ion, and 112 water molecules in the asymmetric unit. No electron density was observed for Gly0, residues 1–4, or residue 311. TyrA is a two-domain, α + β protein (Fig. 1). The protein can be divided into an N-terminal distal domain (residues 1–155) and a C-terminal proximal domain (residues 156–311). Each domain contains a four-stranded, antiparallel β-sheet sandwiched by α-helices in a ferredoxin-like fold. The two β-sheets pack against each other in a β-barrel arrangement. Both domains contribute to forming the active site of the protein. The N-terminal domain forms one wall of the active site via a loop between β-strand 6 and α-helix 4. The C-terminal domain contributes the majority of residues to the active site and forms a cavity for heme binding between its β-sheet and α-helices 8, 9, and 10. Residues which interact directly with the heme moiety arise from both domains. F1

As in the apo form,[18] the TyrA/heme complex is dimeric, with a predominantly hydrophobic dimerization interface consisting of a loop between β-strands 8 and 9 that penetrates a groove formed by α-helix 3 and β-strand 6, with an additional smaller interface formed by α-helix 6 packing against α-helix 4 of the partner monomer. Structurally related heme-binding proteins exhibit different quaternary structure and include pentamers[16] (1vdh, 1t0t), hexamers (2gvk), and monomers (2d3q).[14] *Bt*DyP has the highest sequence identity to TyrA (33%), and retains the TyrA dimerization interface while further associating into a hexamer (trimer of dimers).[18] Although the physiological role of oligomerization is not known for any of the proteins, the heme-binding sites appear to be conserved and independent of oligomerization.

The electron density maps reveal the location of the bound heme, allowing for unambiguous determination

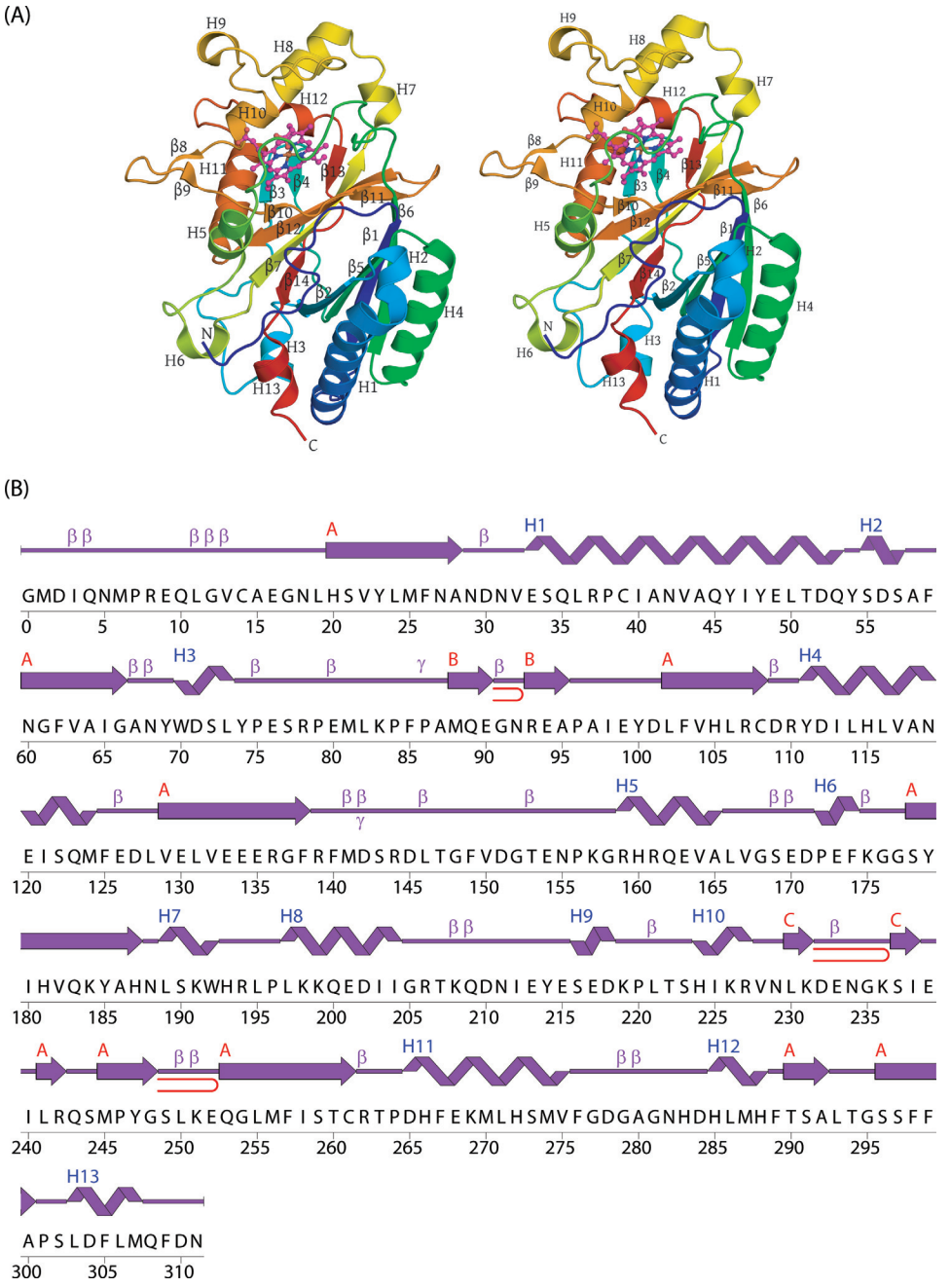

Figure 1

Crystal structure of TyrA/heme complex from Shewanella oneidensis*: (**A**) Stereo ribbon diagram of the TyrA monomer color-coded from N-terminus (blue) to C-terminus (red). Helices 1–13 and β-strands 1–10 are indicated. (**B**) Diagram showing the secondary structural elements of TyrA superimposed on its primary sequence. The α-helices, β-strands, β-turns, and γ-turns are indicated. The β-hairpins are depicted as red loops.*

COLOR

of heme conformation and identification of interacting residues (Fig. 2). The Fe(III) is penta-coordinate and in the plane of the porphyrin, with a bond length of 2.0 Å between the Fe(III) and pyrrole nitrogens. His224 acts as an axial ligand, coordinating the Fe(III) with a bond distance of 2.1 Å. His224 forms a Fe-His-Asp triad with Asp284, a motif seen in the plant peroxidase superfamily.[29] In the plant peroxidases, however, the axial histidine ligand is oriented with the C_α-C_β bond parallel to the heme plane [Fig. 3(A)]. This orientation is thought to be important for constraining the iron in the heme plane and stabilizing the Fe(IV) intermediate.[30] Rotations

J_ID: Z7E Customer A_ID: 21673 Cadmus Art: PROT21673 Date: 28-JUNE-07 Stage: I Page: 5

COLOR

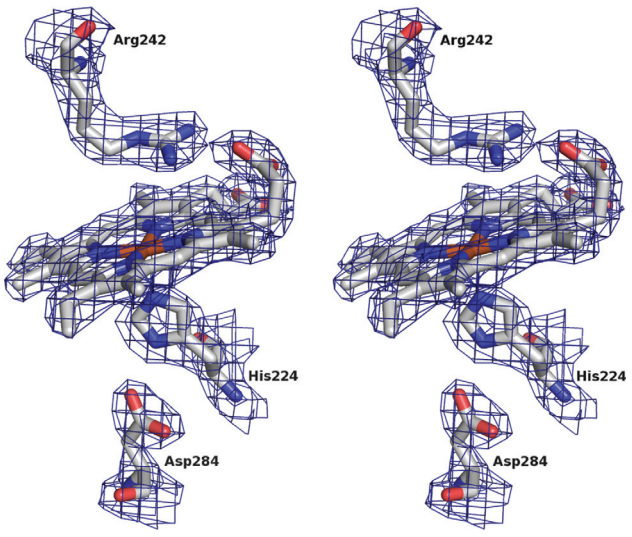

Figure 2

Stereo diagram of $2F_o$-F_c electron density map contoured at 1.5 σ around the bound heme in TyrA: The heme molecule and side chains of residues His224, Arg242, and Asp284 are depicted in ball-and-stick, with carbons (gray), oxygens (red), nitrogens (dark blue), and iron (orange).

about the C_α-C_β bond of His224 in TyrA would allow the side chain to move directly away from the iron center; however, a hydrogen bond between the His224 side chain and Asp284 locks His224 in place. Asp284 is further constrained by hydrogen-bonding interactions with the backbone nitrogens of His285 and Leu286.

The plant peroxidases have an absolutely conserved catalytic histidine that is distal to the heme ligand and ~5 Å from the iron center. This distal histidine helps position a water molecule that occupies the sixth coordination site of the Fe(III). In TyrA, the distal iron coordination site is vacant, with the nearest water molecule 4.2 Å away from the Fe(III). The water molecule is held in place by a hydrogen-bonding network with the carboxylate of Asp151 and hydroxyl of Ser244 [Fig. 3(B)].

Unlike other structurally characterized peroxidases to date, the propionic acid moiety on pyrrole D adopts a highly bent configuration because of a strong hydrogen-bonding network formed between the propionic carboxylate, Arg206, Arg242, a water molecule, and the propionate of pyrrole C. The bent propionate is 2.97 Å from Arg242 and 2.6 Å from a water molecule, which is also hydrogen-bonded to Arg206 at a distance of 2.91 Å. ~~This hydrogen-bonding network forces the propionate to bend almost 90° out of the plane of the porphyrin.~~ The second propionic moiety is sequestered by a hydrogen-bonding network consisting of two water molecules, Arg206, the bent propionate moiety, and Asn298 [Fig. 3(B)].

The region surrounding the heme molecule is rich in hydrophobic residues including Tyr185, Ile204, Val224, Ile225, Phe257, Met 270, Met 274, and Met 287. In addition to binding the hydrophobic porphyrin molecule, the hydrophobic active site likely favors small hydrophobic substrate molecules. While the physiological substrate for TyrA has not been identified, TyrA is annotated as a protein involved in the melanin biosynthesis pathway, and likely substrates include aromatic small molecules.

Comparisons with the apo form of TyrA[18] (PDB accession code 2hag) show little structural change upon heme binding. The RMSD over 306 C_α atoms for the two structures is 0.32 Å. Thus, the active site is primed for heme binding, with no major structural changes necessary for sequestering heme. The most noticeable changes were confined to side-chain orientations in the active site. The side-chain conformations of Glu154, Val228, and Asn229 differ in the two structures to accommodate the heme moiety (Fig. 4). The alternate conformation adopted by Glu154 is necessary to avoid steric clashes with the heme propionate. Asn229 adopts a rotamer that can hydrogen bond with one of the heme proponiate groups. F4

To confirm the catalytic activity of TyrA as a novel heme-binding peroxidase, enzymatic assays were performed with an anthraquinone dye, RB5. While the physiological substrate for TyrA has not been identified, RB5 was chosen as a substrate for measuring peroxidase activity because of the high levels of activity against RB5 seen with a related protein, DyP.[14] The rate of reaction was followed spectrophotometrically by monitoring a decrease in absorbance at 600 nm. As expressed and purified, TyrA exhibited little peroxidase activity in the presence of peroxide and substrate because of only low levels of heme present in the heterologously expressed protein. However, when reconstituted with hemin chloride, peroxidase activity increased dramatically, with a K_m of 84 μ*M* for RB5 and a k_{cat} of 5.9 s^{-1}. The K_m value obtained for TyrA was 1.5 times higher than that reported for DyP, while the k_{cat} was ~50-fold lower.[14] As the reaction conditions were the same for the TyrA and DyP assays, differences in the K_m and k_{cat} most likely reflect different substrate specificity. DyP was shown to be very promiscuous, with activity against a variety of azo, anthraquinone, and phenolic compounds. As the true substrate for TyrA has not been identified, peroxidase activity could be much higher against the physiological substrate under optimized conditions.

Previous biochemical experiments and modeling studies suggested different locations and residues important for heme binding. Our structural results of TyrA in complex with iron(III) protoporphyrin (IX) fully delineates the heme-binding motifs in the DyP family and confirms the importance of His224, an absolutely conserved histidine in all DyP family members.[18] Because of the multiple oligomerization states exhibited by DyP family proteins, it was unclear whether oligomerization affected

ID: jaganm Date: 28/6/07 Time: 17:39 Path: J:/Production/PROT/Vol00000/070247/3B2/C2PROT070247

J_ID: Z7E Customer A_ID: 21673 Cadmus Art: PROT21673 Date: 28-JUNE-07 Stage: I Page: 6

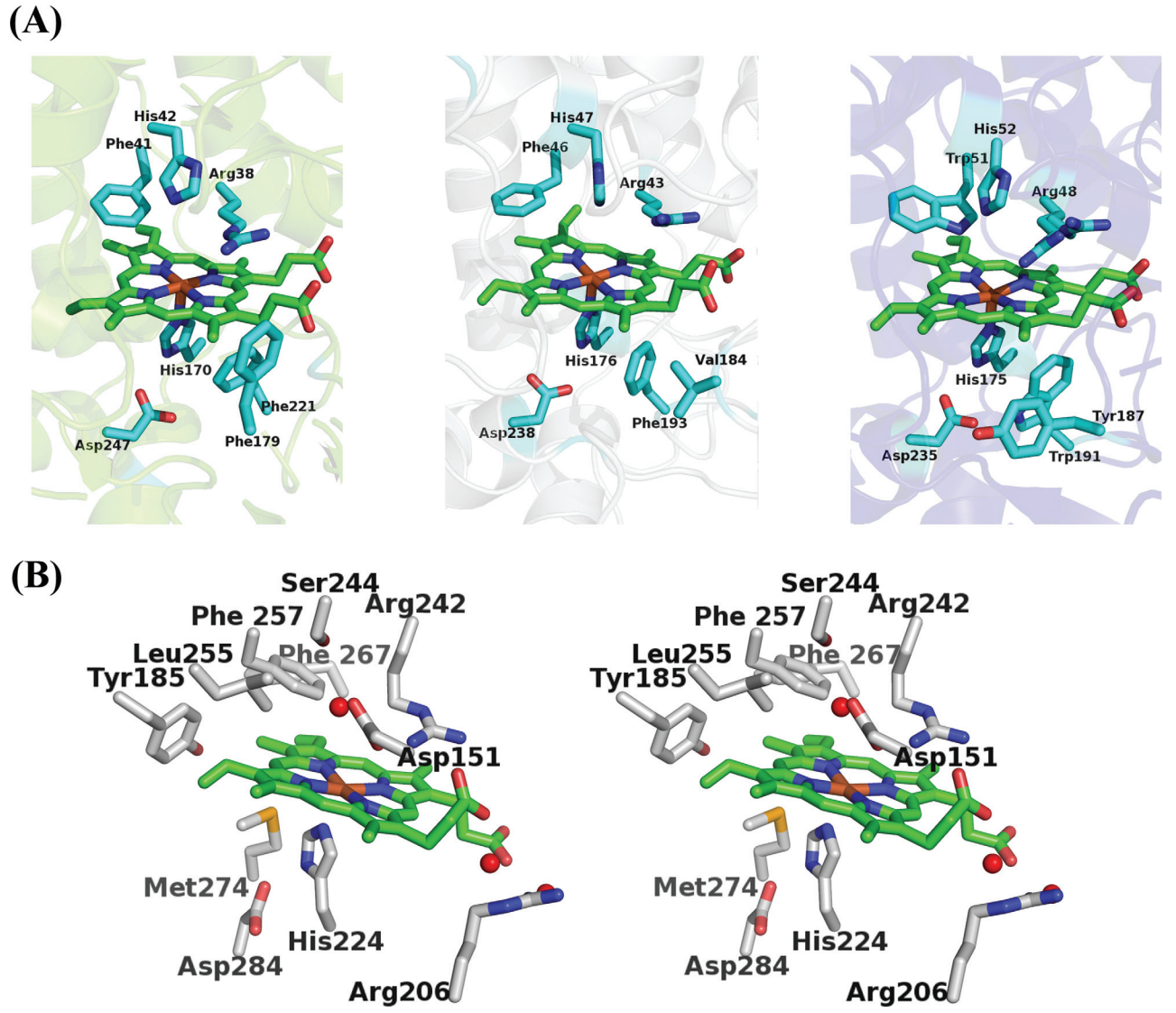

COLOR

Figure 3

*Active sites of representative peroxidases: (**A**) Active site comparison of class I, II, and III plant peroxidases. HRP (left; PDB code 1hch), LiP (middle; PDB code 1llp), and CcP (right; PDB code 1zby) are shown. The heme molecule is colored by atom, with carbons (green), nitrogens (dark blue), oxygens (red), and iron (orange). Side chains are labeled and colored by atom, with carbons in cyan. (**B**) Stereo view of the TyrA heme-binding site, with heme carbons (green) and side chain carbons (grey). Waters are depicted as red spheres.*

heme binding. Previous studies on heme binding in TyrA, *Bt*DyP, and TT1485 all demonstrated ratios less than 1:1 for heme/protein binding, with values ranging from 0.3 to 0.6:1 (heme:protein).[16,18] Based on the well-defined electron density for heme and the low B values, the heme molecule exhibits full occupancy in the active site of TyrA. The independence of heme binding in each monomer is further supported by the location of the active site, which is distal to the oligomerization interface. Taken together, these results demonstrate that each monomer of the dimer is able to independently sequester heme. The difficulty in accurately measuring heme:protein stoichiometry may be due to the low levels of heme present, even in heterologously expressed protein. For example, the apo TyrA and apo *Bt*DyP proteins exhibited a Soret absorbance at 410 nm, and the protein solutions were faintly orange in color, indicating the presence of heme. Poor estimation of initial heme content could account for the low ratio of heme:protein seen in these studies.

The DyP family is an example of functional convergence of heme-dependent peroxidase activity. The ferre-

DOI 10.1002/prot

ID: jaganm Date: 28/6/07 Time: 17:39 Path: J:/Production/PROT/Vol00000/070247/3B2/C2PROT070247

J_ID: Z7E Customer A_ID: 21673 Cadmus Art: PROT21673 Date: 28-JUNE-07 Stage: I Page: 7

COLOR

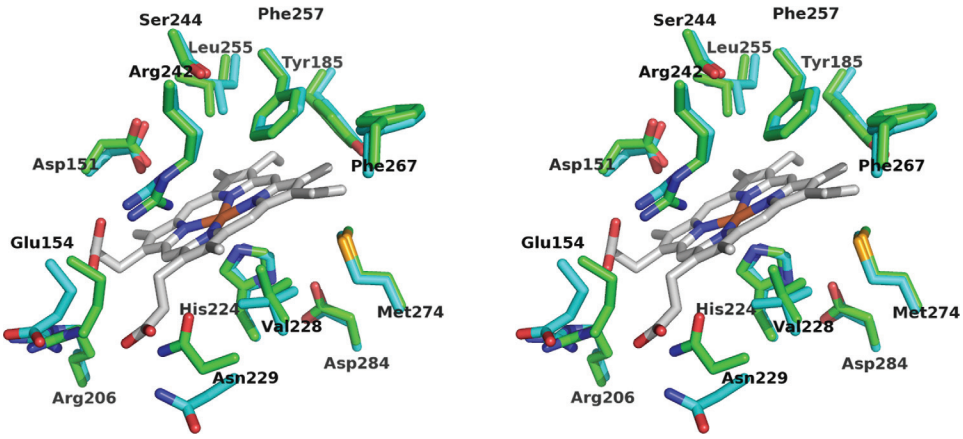

Figure 4

Stereo overlay of the TyrA apo- and heme-bound structures: The apo- (green) and heme-bound (cyan) structures show little conformational change during heme binding.

doxin-like fold was appropriated to bind heme and evolved to have a similar function as the α-helical plant peroxidase fold. Structural comparisons with representative members of the plant peroxidase superfamily underscore the striking differences in tertiary structure. All plant peroxidase superfamily members, including the bacterial and fungal peroxidases, are primarily α-helical proteins. In the plant peroxidases, the distal and proximal α-helical domains contribute equally to the heme-binding site. The binding site cavity is formed by a cleft between α-helices and the core of the protein. In addition, the overall topology of the plant peroxidase

COLOR

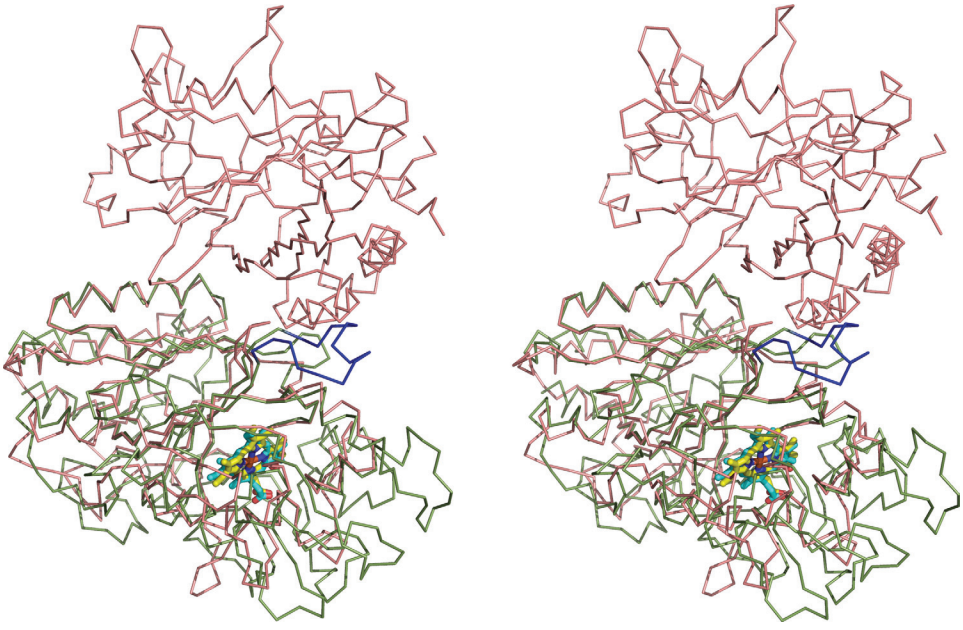

Figure 5

Structural comparison of TyrA and DyP: Ribbon diagram of a structural superposition of DyP (green) on TyrA (pink). TyrA is dimeric, whereas DyP, which contains several additional loop insertions, is monomeric. A loop insertion in DyP (colored blue) adjacent to the dimerization interface appears to disrupt oligomerization. The heme groups of DyP (yellow) and TyrA (cyan) adopt a similar conformation.

DOI 10.1002/prot

ID: jaganm Date: 28/6/07 Time: 17:39 Path: J:/Production/PROT/Vol00000/070247/3B2/C2PROT070247

J_ID: Z7E Customer A_ID: 21673 Cadmus Art: PROT21673 Date: 28-JUNE-07 Stage: I Page: 8

fold is highly conserved between classes. For example, overlaying the structures of LiP (class II) with HRP (class III) produces an RMSD of 1.85 Å over 216 C_α atoms, and superimposing yeast cytochrome C (class I) with HRP gives an RMSD of 1.65 Å over 213 C_α atoms. In TyrA, the heme-binding site is formed predominantly by the proximal domain of the protein, with only a loop contributed from the distal domain. The β-sheet of the ferredoxin-like fold of the proximal domain helps form a cavity for heme binding, unlike the α-helical cleft between domains seen in all plant peroxidase superfamily structures known to date. Thus, TyrA, which exhibits a ferredoxin-like fold, does not align structurally with the plant peroxidases, and is evolutionarily unrelated to any structural characterized plant peroxidase.

Just as the tertiary structure of TyrA differs from that of the plant peroxidase superfamily, the heme-binding motifs and residues involved in heme sequestering are unique. Specific interactions between the protein and the heme molecule within the plant peroxidase superfamily include an essential arginine and conserved distal and proximal histidine residues, with the proximal histidine forming a Fe-His-Asp triad. While the proximal histidine is conserved in TyrA, the distal histidine is absent. This site is vacant, with the closest water molecule over 4 Å away. The residue most likely to perform the same function as the distal histidine by acting as a proton acceptor for bound peroxide substrate[5,31] is Asp151, which is 4.7 Å away from the iron center. Asp151 may mimic a glutamate residue in chloroperoxidase (CPO) that acts as an acid/base catalyst during generation of Compound I.[32,33] Similar to CPO, TyrA is active at low pH, further supporting the role of Asp151 as both a proton acceptor and donor during the heterolytic cleavage of the peroxide oxygen–oxygen bond. The Fe-Asp distance is consistent with reported distances of the distal histidine in plant peroxidase structures and with the Fe-Glu distance in CPO. Site-directed mutagenesis will be necessary to confirm the role of Asp151 in catalysis.

The propionic acid moieties have an extended conformation in plant peroxidases. In TyrA, the propionate moiety on pyrrole D adopts a bent conformation because of a strong hydrogen-bonding interaction with Arg242. This kinked conformation of one of the propionic acid moieties is not seen in any available heme peroxidase structures to date. Arg242 occupies the distal arginine site important for catalysis in plant peroxidases. In HRP, for example, the distal arginine modulates the pK_a of the catalytic histidine residue by lowering its pK_a, and acts to stabilize the negative charge on the anionic peroxide ligand.[5] In TyrA, Arg242, in addition to hydrogen-bonding to the propionate moiety of pyrrole D, may fulfil this role of anionic peroxide stabilization.

A structural comparison of TyrA with DyP in complex with heme (PDB: 2d3q) shows conservation of the

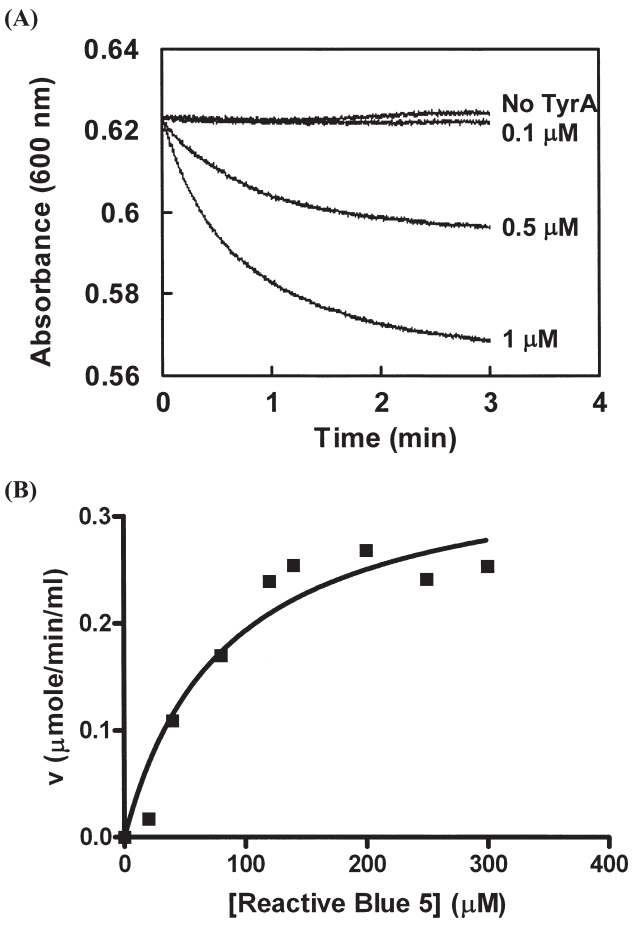

Figure 6

*Enzymatic activity of TyrA: (**A**) Continuous decrease in absorbance at 600 nm was observed in the presence of TyrA. Plot shows raw data obtained in the absence and presence (0.1, 0.5, and 1 μM) of TyrA. (**B**) Michaelis-Menten plot showing the activity of TyrA at different concentrations of RB5. K_m was determined by nonlinear regression analysis using GraphPad Prism software.* AQ7

heme-binding motifs and heme conformation (Fig. 5). F5
Active site residues are highly conserved, including the axial histidine and Fe-His-Asp triad. Conservative amino acid changes include Tyr185 (TyrA)/Phe223 (DyP), Met274 (TyrA)/Ile394 (DyP), and Asp284 (TyrA)/Glu391 (DyP). All other active site residues and the bent heme conformation were identical in both TyrA and DyP, demonstrating conservation in active site topology and architecture.

DyP is monomeric and approximately 150 residues long than TyrA. While the core fold of the proteins is the same, DyP has a number of loop insertions in its C-terminal domain. These insertions do not affect the active site; however, they do disrupt the dimerization interface seen in TyrA. We previously postulated that the insertions in DyP might influence its oligomerization state, as the insertions were adjacent to the TyrA and *Bt*DyP

DOI 10.1002/prot

ID: jaganm Date: 28/6/07 Time: 17:40 Path: J:/Production/PROT/Vol00000/070247/3B2/C2PROT070247

dimerization interfaces.[18] Structural comparison of TyrA and DyP supports this hypothesis, as the dimer-forming loop between β-strands 8 and 9 in TyrA is approximately 10 residues longer and forms a small α-helix (Fig. 5; colored blue) in DyP.

CONCLUSIONS

This study has provided a high-resolution structure of a DyP peroxidase in complex with heme. Based on our data and other structural studies,[16,17] the tertiary structure of the DyP family and motifs important for heme binding have been elucidated. The heme iron is pentacoordinate, with the protein contributing a histidine ligand (His224) to the iron center. Asp151 most likely acts as a proton donor/acceptor during generation of Compound I, and takes the place of the catalytic histidine used by plant peroxidases. This Asp substitution helps explain why the DyP family is active at low pH.[14,15] Analogous to the catalytic Glu in CPO, the catalytic Asp would be a better proton donor at lower pH. Unlike other structurally characterized peroxidases to date, the propionate moiety of pyrrole D adopts a novel bent conformation due to a hydrogen-bonding interaction with Arg242. The coordinates of DyP in complex with heme further support our identification of residues important for heme binding and the hypothesis that the bent propionate moiety is characteristic of the DyP family of peroxidases.

Sequence and structural comparisons to the plant and animal peroxidase superfamilies demonstrate that the DyP family cannot be classified within either superfamily. The DyP family likely evolved from a different ancestral gene, and is an example of convergent evolution of peroxidase function. Examination of related sequences demonstrates that the DyP protein family spans the bacterial, fungal, and archaeal kingdoms. As the DyP family is well represented in prokaryotes, as well as fungi, we propose that a new peroxidase superfamily be added to encompass the DyP peroxidases.

ACKNOWLEDGMENTS

Portions of this research were carried out at the Stanford Synchrotron Radiation Laboratory (SSRL). The SSRL is a national user facility operated by Stanford University on behalf of the U.S. Department of Energy, Office of Basic Energy Sciences. The SSRL Structural Molecular Biology Program is supported by the Department of Energy, Office of Biological and Environmental Research, and by the National Institutes of Health (National Center for Research Resources, Biomedical Technology Program, and the National Institute of General Medical Sciences). Fellowship received from the National Foundation for Cancer Research to PS.

REFERENCES

1. Welinder KG, Mauro JM, Norskov-Lauritsen L. Structure of plant and fungal peroxidases. Biochem Soc Trans 1992;20:337–340.
2. Furtmuller PG, Zederbauer M, Jantschko W, Helm J, Bogner M, Jakopitsch C, Obinger C. Active site structure and catalytic mechanisms of human peroxidases. Arch Biochem Biophys 2006;445:199–213.
3. Taurog A. Molecular evolution of thyroid peroxidase. Biochimie 1999;81:557–562.
4. Teixeira FK, Menezes-Benavente L, Margis R, Margis-Pinheiro M. Analysis of the molecular evolutionary history of the ascorbate peroxidase gene family: inferences from the rice genome. J Mol Evol 2004;59:761–770.
5. Hiner AN, Hernandez Ruiz J, Arnao MB, Rodriguez Lopez JN, Garcia Canovas F, Acosta M. Complexes between *m*-chloroperoxybenzoic acid and horseradish peroxidase compounds I and II: implications for the kinetics of enzyme inactivation. J Enzyme Inhib Med Chem 2002;17:287–291.
6. Gold MH, Kuwahara M, Chiu AA, Glenn JK. Purification and characterization of an extracellular H_2O_2-requiring diarylpropane oxygenase from the white rot basidiomycete, *Phanerochaete chrysosporium*. Arch Biochem Biophys 1984;234:353–362.
7. Sundaramoorthy M, Kishi K, Gold MH, Poulos TL. The crystal structure of manganese peroxidase from *Phanerochaete chrysosporium* at 2.06 Å resolution. J Biol Chem 1994;269:32759–32767.
8. Duroux L, Welinder KG. The peroxidase gene family in plants: a phylogenetic overview. J Mol Evol 2003;57:397–407.
9. Bakalovic N, Passardi F, Ioannidis V, Cosio C, Penel C, Falquet L, Dunand C. PeroxiBase: a class III plant peroxidase database. Phytochemistry 2006;67:534–539.
10. Lang G, Spartalian K, Yonetani T. Mossbauer spectroscopic study of compound ES of cytochrome c peroxidase. Biochim Biophys Acta 1976;451:250–258.
11. Browlett WR, Stillman MJ. Evidence for heme pi cation radical species in compound I of horseradish peroxidase and catalase. Biochim Biophys Acta 1981;660:1–7.
12. Kaneko Y, Tamura M, Yamazaki I. Formation of porphyrin pi cation radical in zinc-substituted horseradish peroxidase. Biochemistry 1980;19:5795–5799.
13. Yonetani T, Ray GS. Studies on cytochrome c peroxidase. III. Kinetics of the peroxidatic oxidation of ferrocytochrome c catalyzed by cytochrome c peroxidase. J Biol Chem 1966;241:700–706.
14. Kim SJ, Shoda M. Decolorization of molasses and a dye by a newly isolated strain of the fungus *Geotrichum candidum* Dec 1. Biotechnol Bioeng 1999;62:114–119.
15. Johjima T, Ohkuma M, Kudo T. Isolation and cDNA cloning of novel hydrogen peroxide-dependent phenol oxidase from the basidiomycete *Termitomyces albuminosus*. Appl Microbiol Biotechnol 2003;61:220–225.
16. Ebihara A, Okamoto A, Kousumi Y, Yamamoto H, Masui R, Ueyama N, Yokoyama S, Kuramitsu S. Structure-based functional identification of a novel heme-binding protein from *Thermus thermophilus* HB8. J Struct Funct Genomics 2005;6:21–32.
17. Sato T, Hara S, Matsui T, Sazaki G, Saijo S, Ganbe T, Tanaka N, Sugano Y, Shoda M. A unique dye-decolorizing peroxidase, DyP, from *Thanatephorus cucumeris* Dec 1: heterologous expression, crystallization and preliminary X-ray analysis. Acta Crystallogr D Biol Crystallogr 2004;60:149–152.
18. Zubieta C, Krishna SS, Kapoor M, Kozbial P, McMullan D, Axelrod HL, Miller MD, Abdubek P, Ambing E, Astakhova T, Carlton D, Chiu HJ, Clayton T, DiDonato M, Duan L, Elsliger MA, Feuerhelm J, Grzechnik SK, Hale J, Hampton E, Han GW, Jaroszewski L, Jin KK, Klock HE, Knuth MW, Koesema E, Kumar A, Marciano D, Morse AT, Nigoghossian E, Okach L, Oommachen S, Reyes R, Rife CL, Schimmel P, Van den Bedem H, Weekes D, White A, Xu Q, Hodgson KO, Wooley J, Deacon AM, Godzik A, Lesley SA, Wilson IA. Crystal structures of two novel dye-decolorizing peroxidases

reveal a β-barrel fold with a conserved heme-binding motif. Proteins 2007.
19. Chance M, Powers L, Poulos T, Chance B. Cytochrome c peroxidase compound ES is identical with horseradish peroxide compound I in iron-ligand distances. Biochemistry 1986;25:1266–1270.
20. Sturm A, Schierhorn A, Lindenstrauss U, Lilie H, Bruser T. YcdB from *Escherichia coli* reveals a novel class of Tat-dependently translocated hemoproteins. J Biol Chem 2006;281:13972–13978.
21. Lovell SC, Davis IW, Arendall WB, 3rd, de Bakker PI, Word JM, Prisant MG, Richardson JS, Richardson DC. Structure validation by Cα geometry: π, ψ and Cβ deviation. Proteins 2003;50:437–450.
22. The CCP4 suite: programs for protein crystallography. Acta Crystallogr D Biol Crystallogr 1994;50:760–763.
23. Kabsch W. Automatic processing of rotation diffraction data from crystals of initially unknown symmetry and cell constants. J Appl Cryst 1993;26:795–800.
24. Storoni LC, McCoy AJ, Read RJ. Likelihood-enhanced fast rotation functions. Acta Crystallogr D Biol Crystallogr 2004;60:432–438.
25. Emsley P, Cowtan K. Coot: model-building tools for molecular graphics. Acta Crystallogr D Biol Crystallogr 2004;60:2126–2132.
26. Winn MD, Murshudov GN, Papiz MZ. Macromolecular TLS refinement in REFMAC at moderate resolutions. Methods Enzymol 2003;374:300–321.
27. Yang H, Guranovic V, Dutta S, Feng Z, Berman HM, Westbrook JD. Automated and accurate deposition of structures solved by X-ray diffraction to the Protein Data Bank. Acta Crystallogr D Biol Crystallogr 2004;60:1833–1839.
28. Vriend G. Parameter relation rows: a query system for protein structure function relationships. Protein Eng 1990;4:221–223.
29. Goodin DB, McRee DE. The Asp-His-Fe triad of cytochrome c peroxidase controls the reduction potential, electronic structure, and coupling of the tryptophan free radical to the heme. Biochemistry 1993;32:3313–3324.
30. Finzel BC, Poulos TL, Kraut J. Crystal structure of yeast cytochrome c peroxidase refined at 1.7-A resolution. J Biol Chem 1984;259:13027–13036.
31. Fulop V, Phizackerley RP, Soltis SM, Clifton IJ, Wakatsuki S, Erman J, Hajdu J, Edwards SL. Laue diffraction study on the structure of cytochrome c peroxidase compound I. Structure 1994;2:201–208.
32. Sundaramoorthy M, Terner J, Poulos TL. Stereochemistry of the chloroperoxidase active site: crystallographic and molecular-modeling studies. Chem Biol 1998;5:461–473.
33. Wagenknecht HA, Woggon WD. Identification of intermediates in the catalytic cycle of chloroperoxidase. Chem Biol 1997;4:367–372.

DOI 10.1002/prot

AQ1: Kindly check whether the superscript indicators marked against each author name and the affiliations are OK as typeset.

AQ2: Kindly provide more details regarding your affiliation: location, city, zip code, etc.

AQ3: Please note that the references has been renumbered in order to make sequential as references are cited in table.

AQ4: Kindly provide the volume number and page range for this reference.

AQ5: Kindly check whether the grant information is OK as typeset.

AQ6: JCSG has been deleted from the corresponding information OK?

AQ7: Figure 6 is not cited anywhere in the text. Kindly insert its citation at an appropriate place.